

Chapter 8

Calibration Techniques for Non-contacting Force Excitation

Part 2: Time Domain Methods

Tina Dardeno and Peter Avitabile

Abstract Experimental characterization of the higher frequency modes of a structure presents challenges due to the frequency limitations of traditional excitation techniques. Non-contact excitation via low power ultrasonic transducer presents the possibility of exciting higher frequencies not currently possible with shakers or impact hammers. However, quantification of the actual force applied by the ultrasonic transducer requires that a relationship between the ultrasonic pressure field and the voltage driving the transducer be established.

Part 1 of this paper described calibration methods using frequency domain techniques. Part 2 of this paper, described herein, explores time domain calibration methods using conventional instrumentation before extending the techniques to the ultrasonic transducer. Time domain methods of calibration in the context of this paper involve: (1) prediction of a response for a given excitation using analytical and experimental models; and (2) determination of the sensitivity of an uncalibrated force transducer. Specifically, an analytical model based on the principles of mode superposition is shown to accurately predict the response of a structure to a digitized excitation. Furthermore, if the response of a structure due to an uncalibrated force is plotted against that due to a calibrated force, the slope of the line can be used to determine the sensitivity of the uncalibrated force transducer.

Keywords Non-contact excitation • High frequency excitation • Non-intrusive excitation • Ultrasonic transducer • Calibration methods

8.1 Introduction

Use of ultrasonic waves is being explored as a means by which higher frequency modes of a test article may be characterized without the need for direct contact. Traditional excitation via impact hammers and shakers permits measurement of the force applied to a test article by measuring the voltage output from a force gage, but no analogous mechanism exists for the ultrasonic transducer, which produces an ultrasonic pressure field that is dependent upon the voltage driving the transducer. While some ultrasonic transducers produce an ultrasonic field which acts over a wide area, certain transducers focus the ultrasonic pressure field over an area small enough to be approximated as a discrete point. The question then arises as to how the effective force acting at the focal point can be related to the voltage driving the ultrasonic transducer.

The time domain method of ultrasonic transducer calibration is being developed to complement frequency domain techniques [1]. This method, which utilizes the principle of mode superposition to compute the response of a structure to a digitized excitation, has the benefit of being customizable to even very high frequencies. Furthermore, this method can compute the response of a structure to single or multiple-frequency excitations. To validate the time domain method of transducer calibration, testing was performed using a hammer of known calibration.

8.2 Physical System and Models Developed

A previously designed and fabricated aluminum cantilever structure was used throughout the analyses. The structure is comprised of a cantilever beam with a mass at the base to approximate a built-in condition (Fig. 8.1).

T. Dardeno (✉) • P. Avitabile

Structural Dynamics and Acoustic Systems Laboratory, University of Massachusetts Lowell, One University Avenue, Lowell, MA 01854, USA
e-mail: tina_dardeno@student.uml.edu

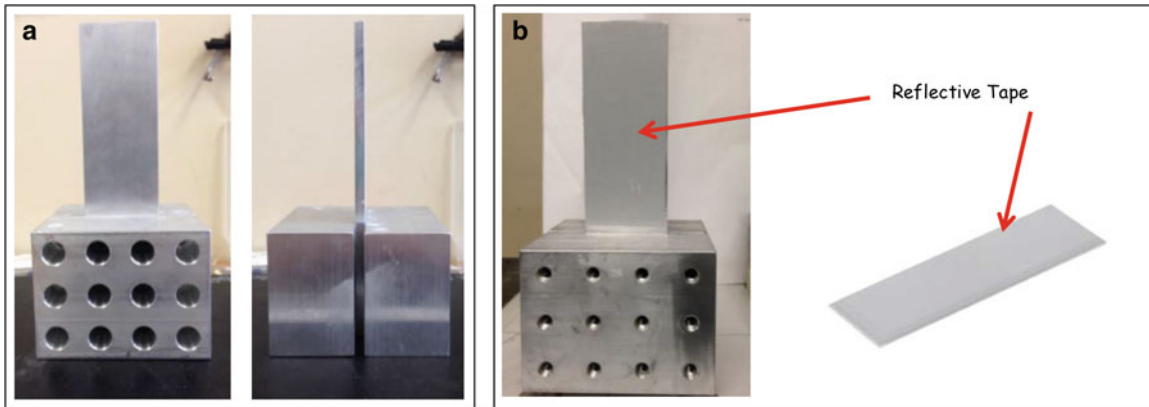


Fig. 8.1 (a) Cantilever calibration structure; (b) Structure with reflective tape applied

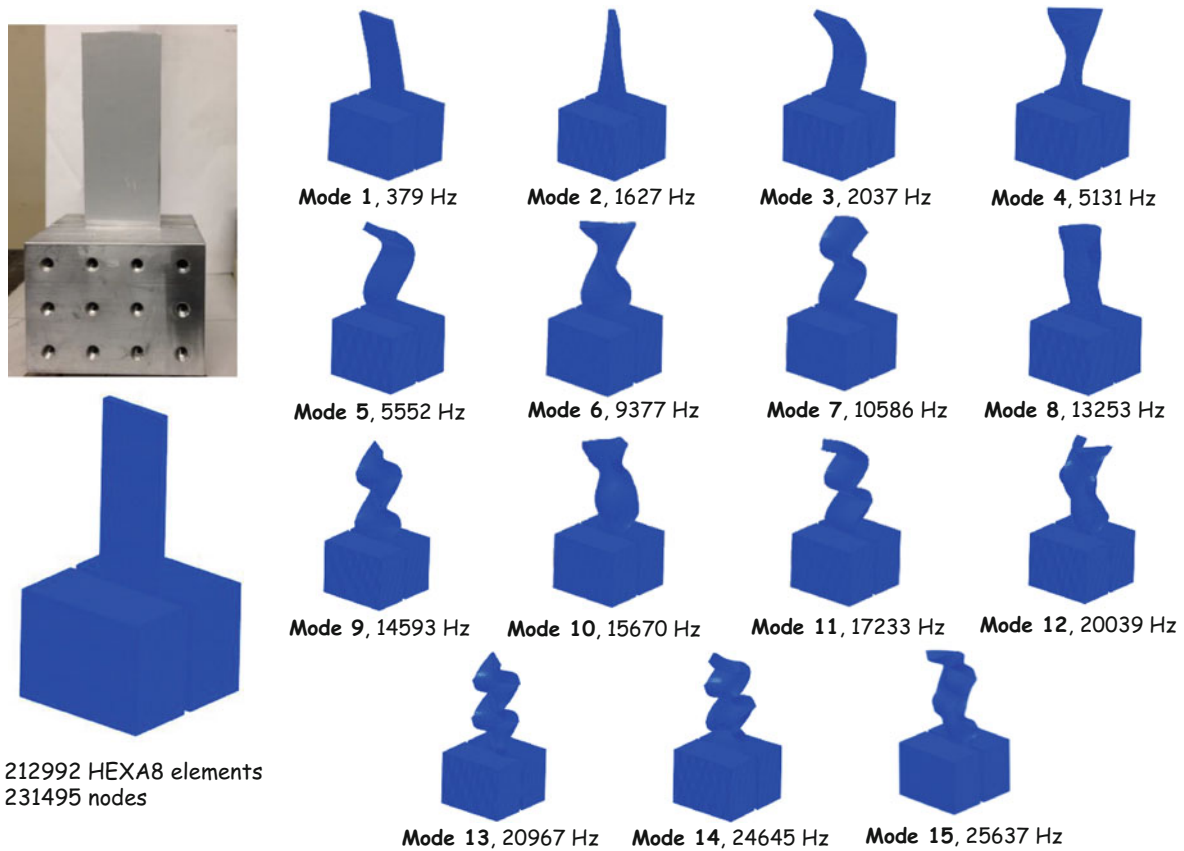


Fig. 8.2 Cantilever model and out-of-plane mode shapes

This structure was designed to mimic turbine blade qualification tests and with dimensions and material properties to generate high frequency mode shapes for calibration of the ultrasonic transducer. To improve laser signal for testing, reflective tape was applied to the face of the structure. The structure was modeled in FEMAP as a plate mounted to a large mass with a refined mesh of eight-noded bricks as shown in Fig. 8.2 [2]. The eigensolution was performed in FEMtools version 3.8 [3]. Only out-of-plane cantilever shapes were considered as no in-plane or base measurements were obtained.

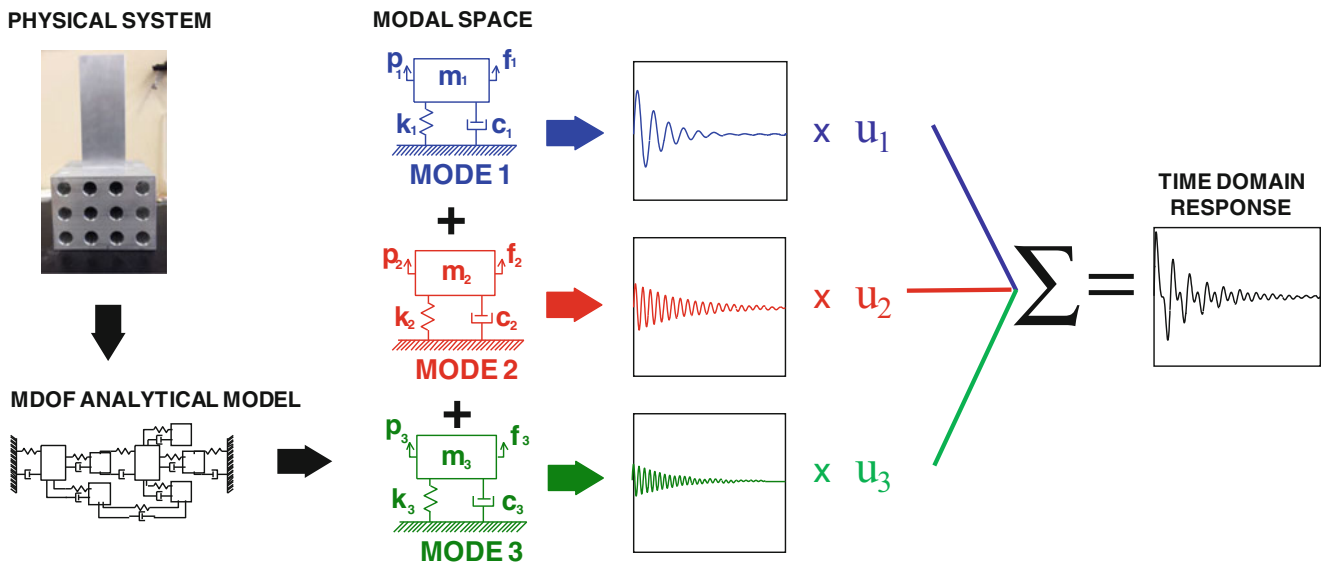


Fig. 8.3 Schematic of mode superposition approach

8.3 Theoretical Background

The analytical models described herein utilize the method of mode superposition to compute an analytical response to a digitized excitation [4]. The basic approach is schematically shown in Fig. 8.3, where the structural system is decomposed into single degree of freedom modal oscillators and the response of each mode is identified. The response is then expanded from the modal response to the physically distributed response on the structure for each mode which is then summed to identify the total response of the system.

The principle of mode superposition described in Fig. 8.3 can be used to estimate the response of a physical system to an actual force excitation. First, frequencies and damping are obtained via experimental frequency response spectra, which are then used to generate mass, stiffness, and damping matrices in modal space. Next, mode shapes corresponding to the test point(s) can be obtained through test or a reliable finite element model. Digitized, instantaneous time data is obtained via test, and the digitized force excitation is transformed to modal space to identify the force contribution of each modal oscillator. The Newmark direct integration method is then used to solve the differential equations of motion for each modal oscillator. The response contribution of each modal oscillator in modal space is then scaled using the corresponding mode shape and summed to compute the total system physical response at a given point. This computed response can be compared to the measured response using overlay and response correlation metrics such as TRAC, as shown in Fig. 8.4. These computations are performed using scripts and functions generated in MATLAB [5].

This response estimation method can be expanded to include transducer calibration. A digitized excitation is obtained; however, an unscaled sensitivity is entered into the channel setup. The response is then computed using a numerical integration scheme. A calibration curve can then be generated by plotting the measured response versus the calculated response and determining the best linear fit of the data. The slope of the line can then be used to compute the sensitivity of the force transducer.

8.4 Characterization of Cantilever Structure

This mode superposition approach requires frequencies, mode shapes, and damping from FEA, test, or both to compute the response. Prior to data collection, measurement point geometry was generated in FEMtools using the sensor placement method of nodal kinetic energy (NKE) and the sensor elimination method of effective independence (EIM) [3]. For computational efficiency, the cantilever calibration structure was modeled as a fixed plate for the pre-test analysis. The test geometry was then exported as a universal file for import into Polytec [6] and LMS [7]. Prior to importing the test geometry into the Polytec data acquisition module [6], 2D and 3D alignments of the laser were performed to align the laser with the measurement points and identify the coordinate system, respectively.

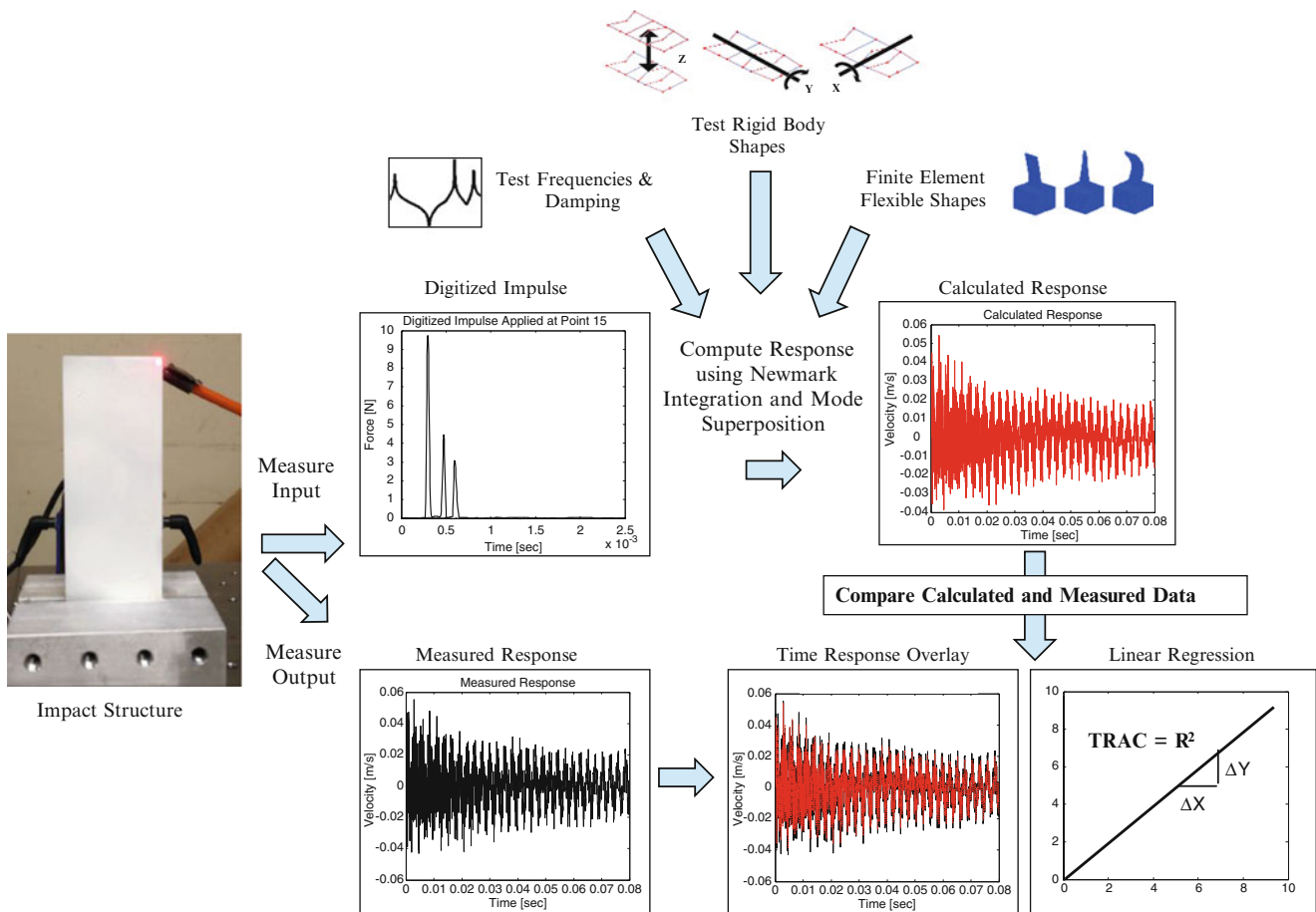


Fig. 8.4 Time response estimation procedure

An impact test was performed to determine the out-of-plane rigid body and flexible modes up to approximately 20 kHz. Figure 8.5 displays the equipment and test geometry used as well as the coherence, input spectrum, and frequency response spectrum at the drive-point. A small metal-tipped hammer was used to excite the structure while velocity measurements were obtained via a single Polytec laser head [6]. Note that the hammer was mounted to a tripod to ensure repeatability of impacts. The hammer remained stationary at point 2645, which is located at the left corner of the free end of the cantilever, while the laser was moved to each measurement point. Point 2645 was selected as the impact location because 2645 was one of the few measurement points that significantly excited all of the target modes. However, point 2645 corresponded to a point of high local flexibility, resulting in many multiple impacts. Five linear averages were taken to minimize error. Data collection was performed in LMS with vibrometer data directly output to the LMS impact testing module [7]. Three rigid body modes and 15 out-of-plane flexible modes were obtained. These shapes were typical for a cantilever plate, as shown in Fig. 8.6. The test results were correlated to the finite element model in FEMtools [3], as shown in Table 8.1. Table 8.1 shows good correlation between model and test, as diagonal MAC values were consistently high for the 15 correlated mode pairs. Furthermore a maximum frequency error of only 4.6 Hz was noted.

8.5 Concept Verification Study Using Hammer of Known Calibration

After determining the frequencies and mode shapes of the structure, time data was collected at point 2671 for response estimation using the LMS spectral testing module [7], as shown in Fig. 8.7. A hammer with a plastic tip (nominal sensitivity 1.99 mV/N) was used to excite the structure at point 2671 to a frequency range less than that excited by the metal tipped hammer. An uncalibrated sensitivity of 1000 mV/N was entered for the hammer into the channel setup. To satisfy requirements of the numerical integration scheme, the smallest possible time step was used for data collection (4.88E-06s).

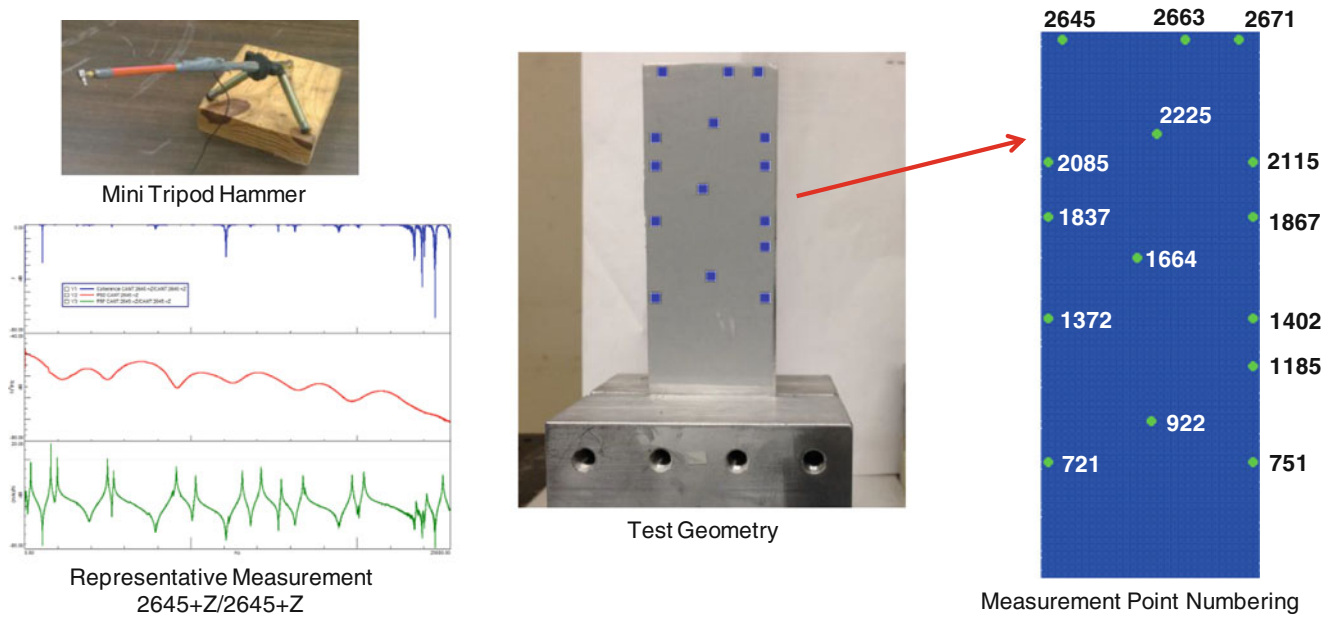


Fig. 8.5 Instrumentation, representative measurement, and measurement point setup for determination of flexible and rigid body mode shapes of cantilever structure

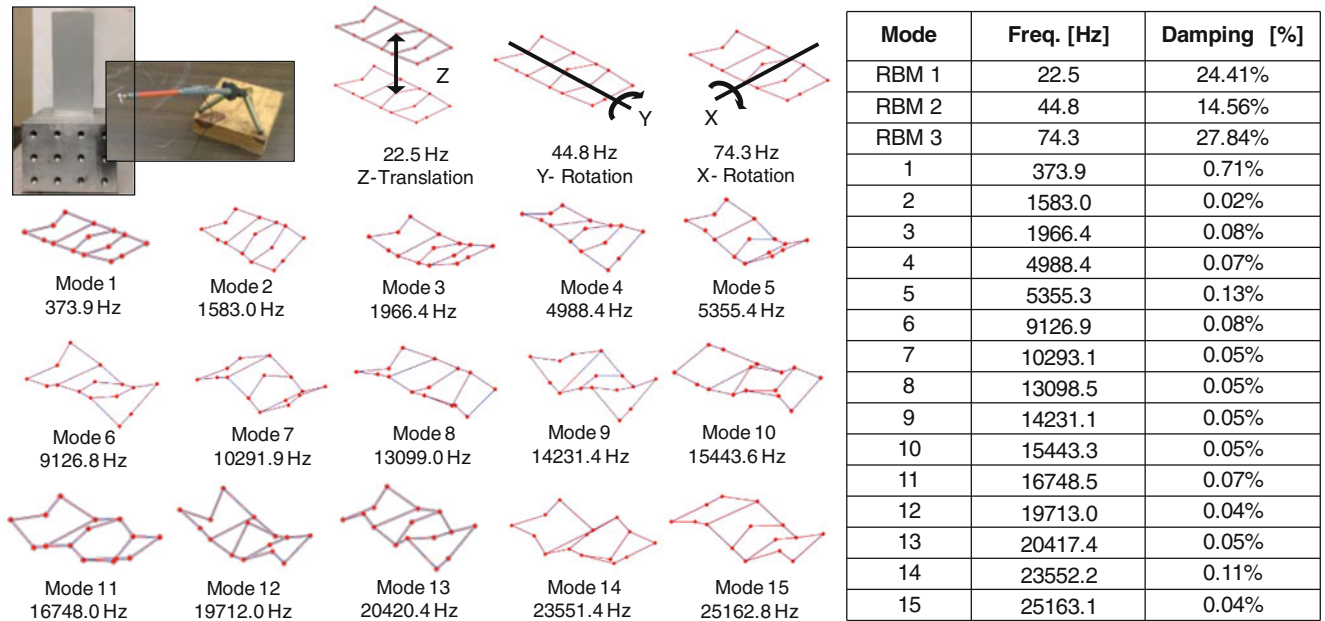


Fig. 8.6 Experimental modal analysis frequencies, damping, and mode shapes

To determine how many flexible modes to include in the calculations, the input auto-spectrum was computed. The spectrum indicated significant excitation up to approximately 10 kHz. Therefore, a total of three rigid body and six flexible modes were included in the analysis (Fig. 8.8).

The digitized impulse, test frequencies, test damping, test rigid body shapes, and finite element flexible shapes from the cantilever and block model were used to compute the unscaled response via mode superposition with Newmark integration. In order to identify the calibration, a plot of the calculated time response versus measured time response will provide an approximate straight line. The sensitivity was then computed via linear regression of the calculated and measured responses, as shown in Fig. 8.9. Then, for better visualization, the calculated response was rescaled using the computed sensitivity, as shown in Fig. 8.10.

Table 8.1 Correlation between finite element and test data

Mode	FEA [Hz]	MAC	EMA [Hz]	% Diff.
1	378.8	99.9	373.9	1.3
2	1626.8	98.6	1583.0	2.8
3	2036.9	98.9	1966.4	3.6
4	5130.8	98.4	4988.4	2.9
5	5552.4	98.2	5355.3	3.7
6	9377.3	99.2	9126.9	2.7
7	10586.0	99.2	10293.1	2.9
8	13253.0	97.0	13098.5	1.2
9	14593.0	99.3	14231.1	2.5
10	15670.0	98.3	15443.3	1.5
11	17233.0	97.6	16748.5	2.9
12	20039.0	97.1	19713.0	1.7
13	20967.0	98.9	20417.4	2.7
14	24645.0	89.4	23552.2	4.6
15	25637.0	95.0	25163.1	1.9

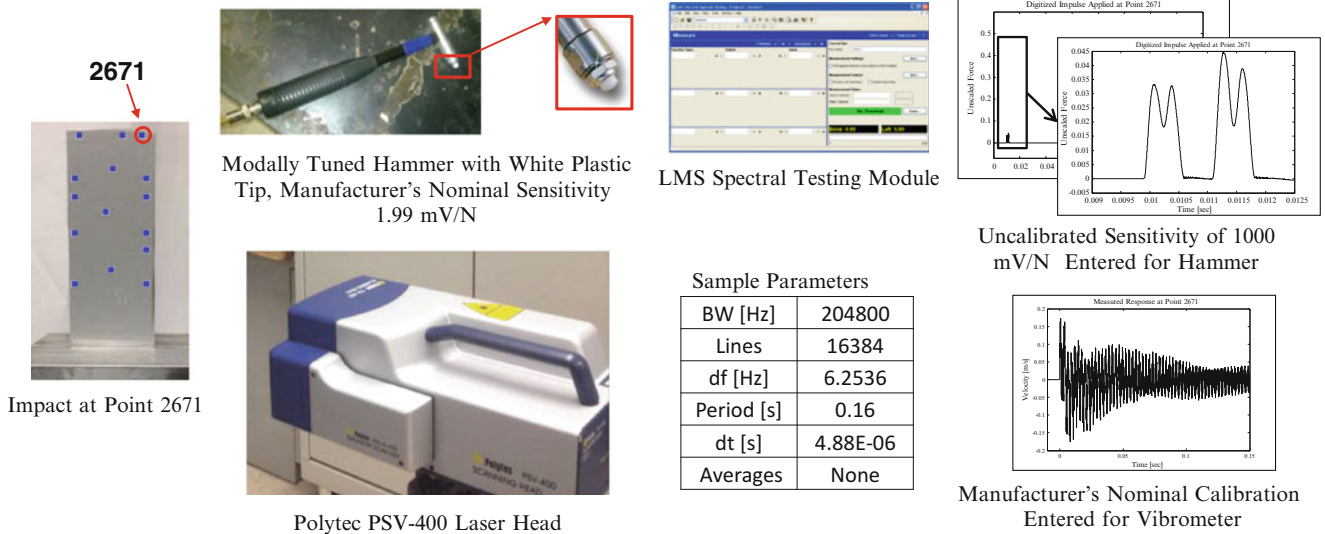
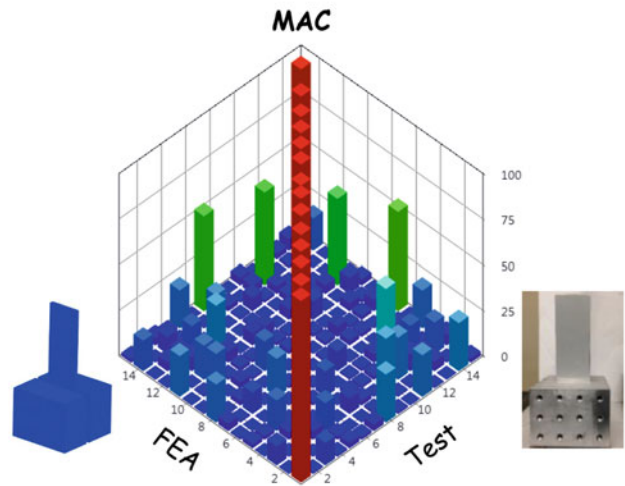


Fig. 8.7 Collection of digitized impulse and time response for hammer calibration

The calculated sensitivity of 2.0066 mV/N is 0.83 % higher than the manufacturer’s nominal sensitivity of 1.99 mV/N. The R^2 value of 0.9570 shows a high correlation between the measured and calculated responses. The results shown are very promising; this time domain approach to force calibration presents a viable way to further validate the calibration values obtained from frequency domain methods.

8.6 Observations

The time domain/mode superposition approach to transducer calibration presented herein appears promising. Several observations related to accuracy of this method were made while performing the analyses. First, because the response is calculated using finite element shapes, model accuracy is crucial. The analysis performed in the previous section utilized a simple fixed cantilever model to develop the pre-test geometry, but extracted shapes from a more detailed model to compute

How many modes to include in the calculated response?

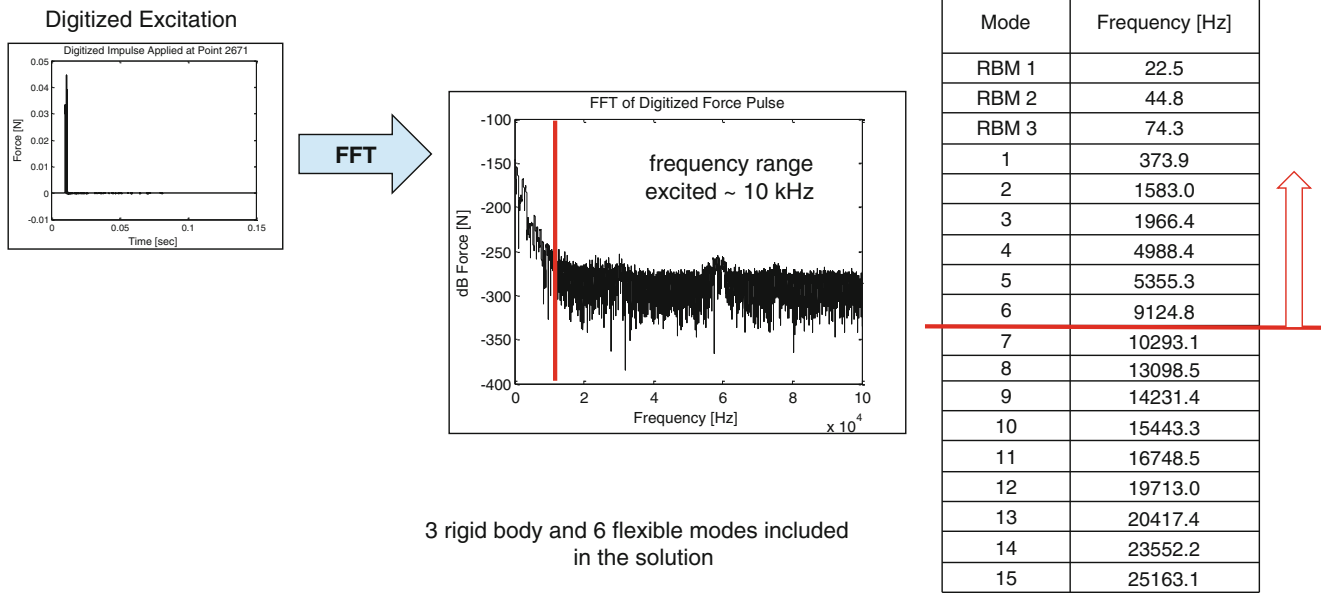


Fig. 8.8 Mode participation in computed response

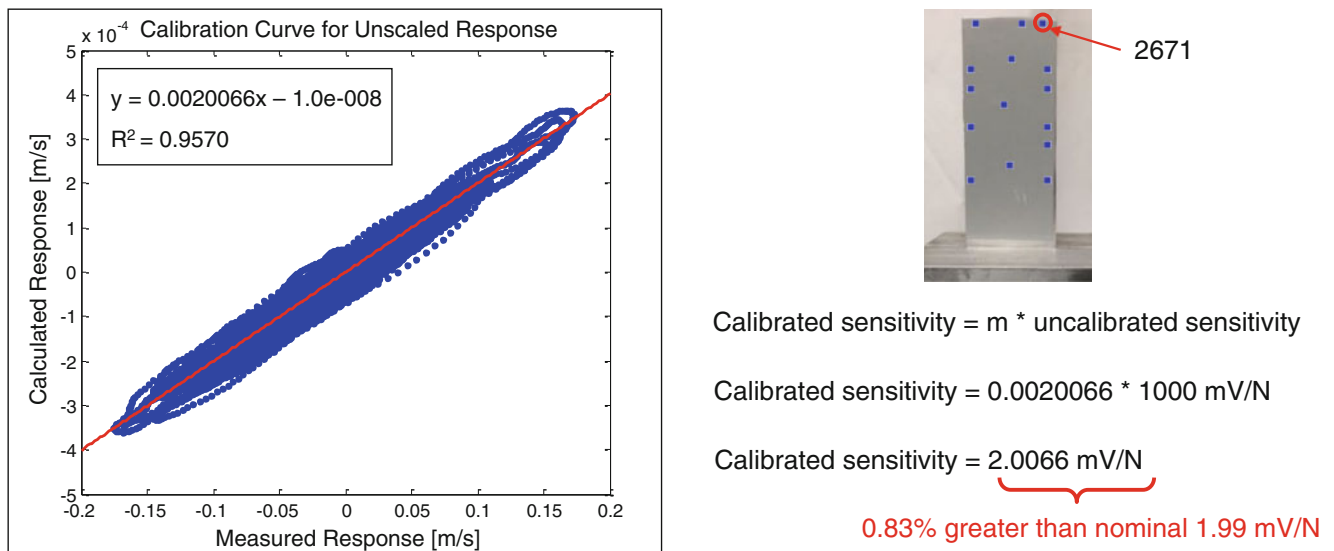


Fig. 8.9 Plot of calculated time response vs. measured time response at point 2671 and calculations to determine hammer calibration value

the response. To demonstrate the importance of the calibration finite element model, the fixed cantilever model is revisited. Figure 8.11 shows the model, shape pairs between the model and test, and correlation results between the model and test.

Figure 8.11 shows that while finite element and test frequencies exhibited some variation, the first six flexible modes demonstrated high diagonal MAC correlation. Test frequencies and finite element mode shapes are used to compute the time response for calibration; therefore, having accurate finite element mode shapes is far more important than having accurate finite element frequencies. Using the finite element shape values from the fixed cantilever model, the transducer sensitivity was recomputed. The original calibration results using shapes from the cantilever and block model are compared to the calibration results using shapes from the fixed cantilever model in Fig. 8.12.

Figure 8.12 shows that both the correlation coefficient and sensitivity value were affected by the model used. The correlation coefficient reduced from 0.9570 to 0.9482 when the response was computed using fixed cantilever shapes. Likewise, the error in the computed sensitivity increased from 0.83 to 12.22 %. Even though the fixed cantilever model

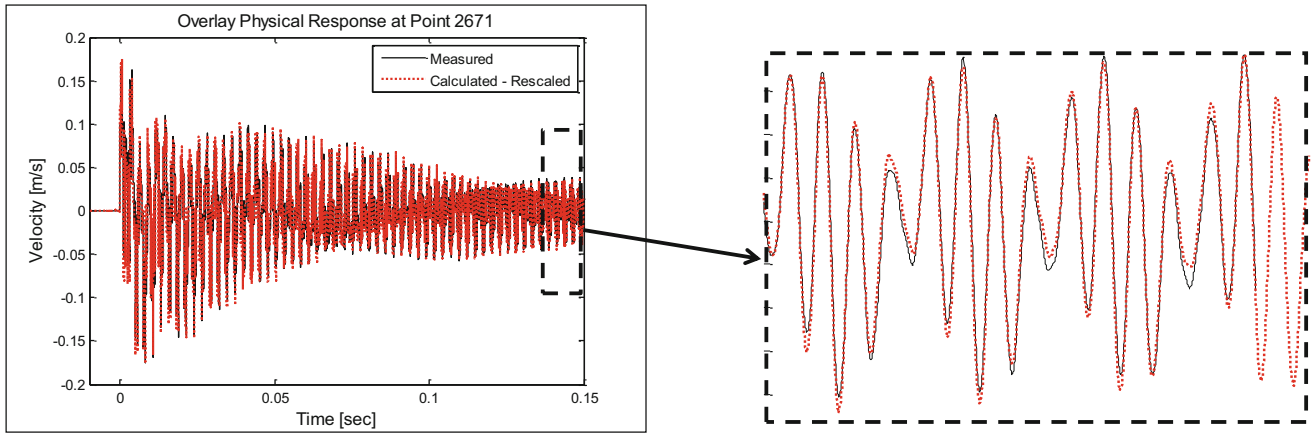


Fig. 8.10 Comparison of measured and rescaled calculated responses at point 2671, cantilever and block model shapes

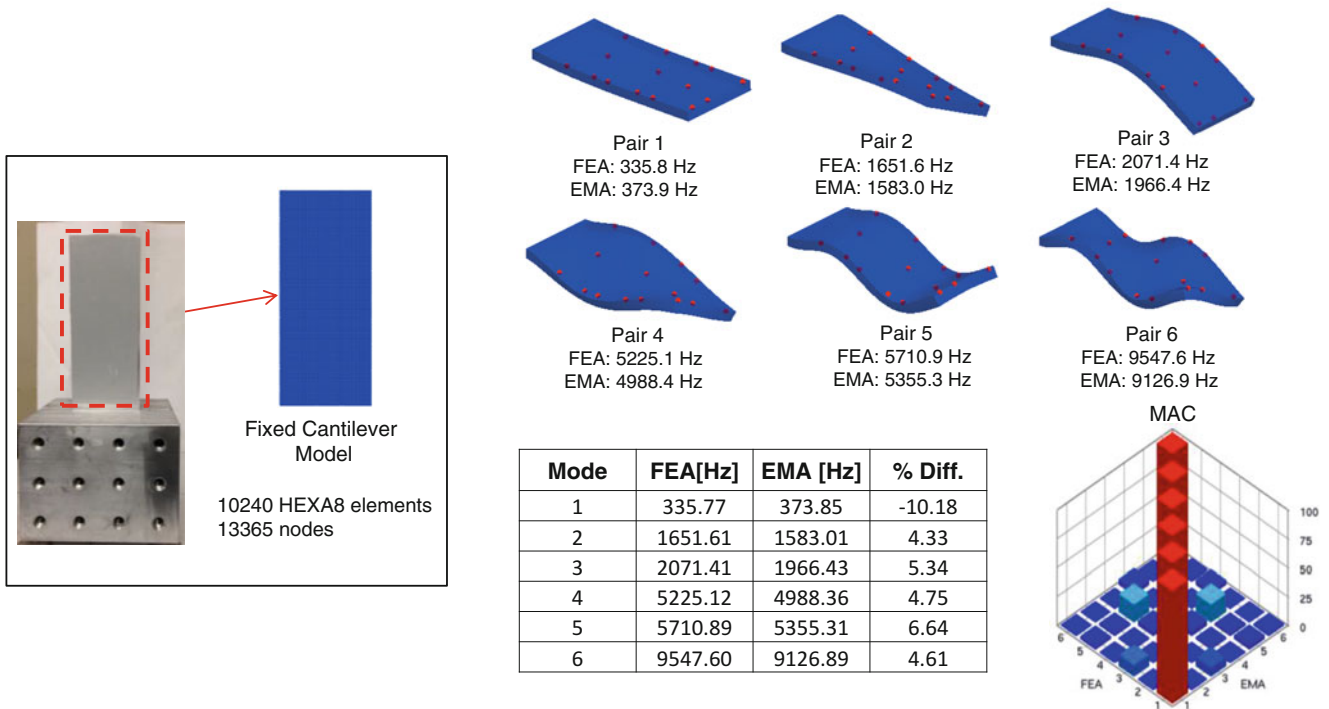


Fig. 8.11 Correlation between test and fixed cantilever model

was shown to correlate highly to the test results via MAC, the local shape values at the measurement location were clearly different for the fixed model compared to the cantilever and block model. These results stress the importance of model accuracy when performing this calibration method.

The second observation is that improper node-point pairing can occur due to discrepancies between test and model coordinates. If the test geometry does not align perfectly with the model, the test points may be paired with finite element nodes that do not share the same dynamic characteristics, as shown in Fig. 8.13.

The cantilever and block model has a distance of 0.0625 in. between each node. Recall that the measurement obtained for input into the mode superposition code was taken at point 2671, which corresponds to the model node shown in Fig. 8.13. This node returns a shape value of 5.32 (normalized to unit modal mass, metric) for the first mode. However, if the model were aligned such that point 2671 was paired with the node directly below (error of 0.0625 in.), the shape value returned would be 5.22. Likewise, if the model were aligned such that point 2671 was paired with two nodes directly below (error of 0.125 in.), the shape value returned would be 5.11. The hammer calibration was recomputed using these nearby nodes, as shown in Fig. 8.14.

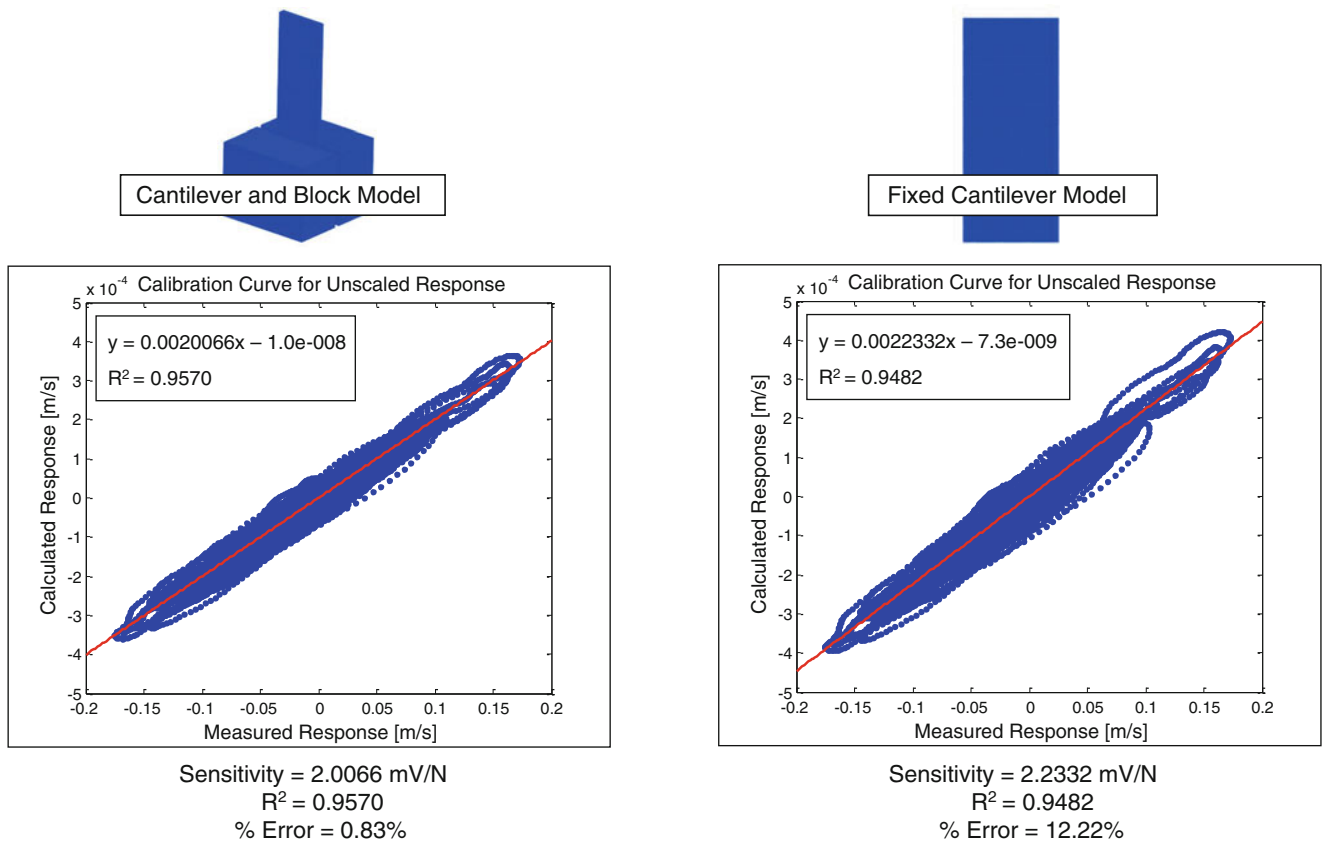


Fig. 8.12 Original hammer calibration results using shapes from cantilever and block model compared to hammer calibration results recomputed using shapes from fixed cantilever model

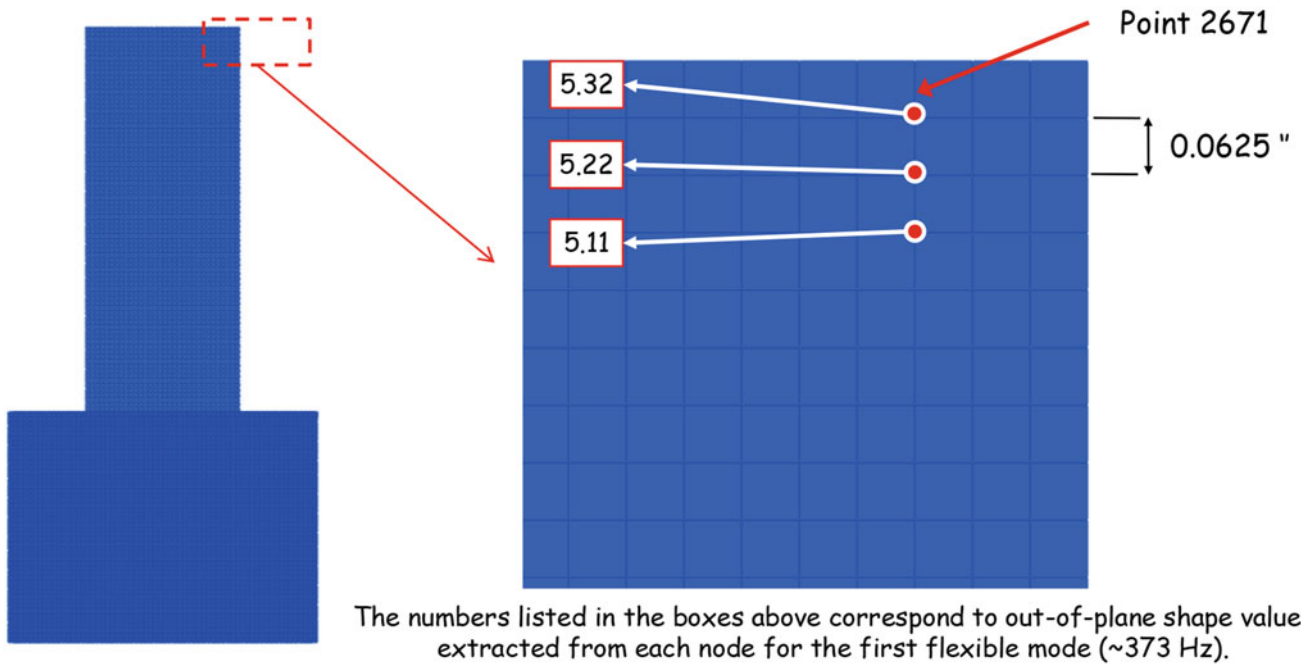


Fig. 8.13 Differences in mode shape values among adjacent nodes

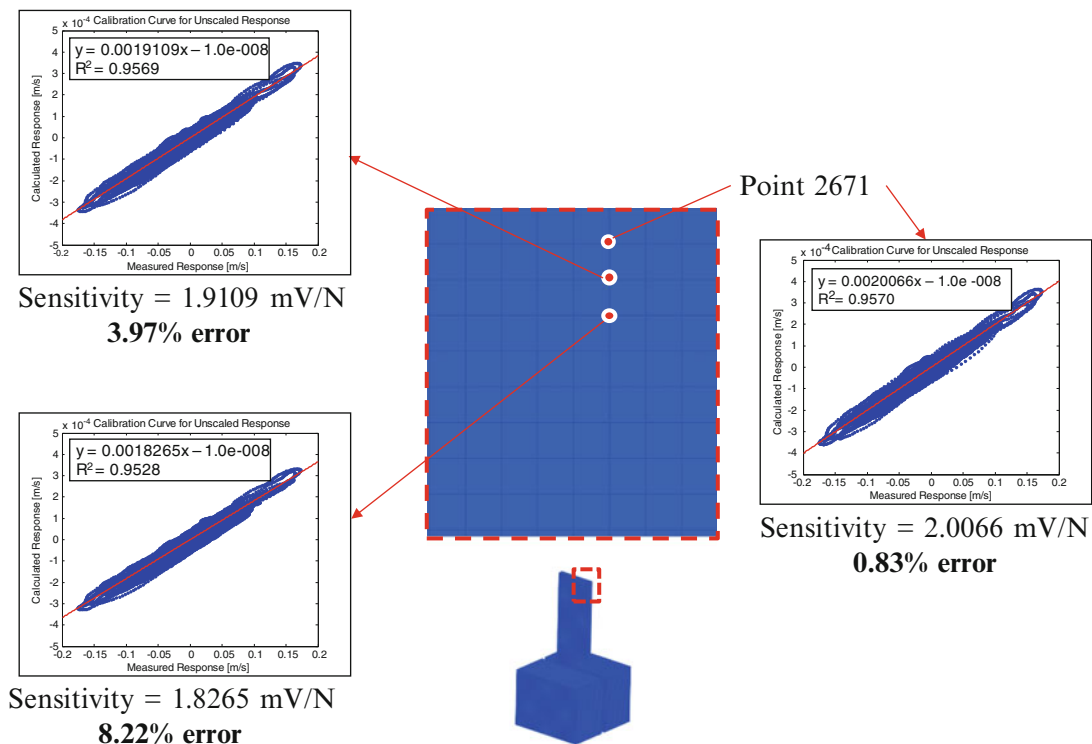


Fig. 8.14 Effect of node-point pairing selection on transducer calibration results

Figure 8.14 shows that an error in node-point pairing can markedly affect the accuracy of the time domain approach to calibration. An error of 0.0625 in. in node placement resulted in an increase from 0.83 % error to 3.97 % error. Likewise, an error of 0.125 in. in node placement increased the error to 8.22 %.

Secondly, Newmark integration has been shown to result in frequency distortion of higher order modes which appears to be related to refinement of the integration time step. As such, other acquisition parameters such as sample rate and window length need to be adjusted to obtain a sufficiently fine time step. When collecting the digitized impulse for this analysis, the parameters were adjusted until the finest possible time step was achieved ($dt = 4.88E-06s$). This required that the maximum sample rate of the system be used. Recall that the response solution included modes up to approximately 10 kHz. Ultrasonic transducers are designed to operate at much higher frequencies, and as such issues may arise when using Newmark integration to compute the response of the structure to an acoustic force. MATLAB's `resample` function is a powerful tool that can be used to prevent the frequency distortion that may result from numerical integration with an insufficient time step. This function resamples uniform or non-uniform data to a new fixed rate and applies a low-pass filter to prevent aliasing [8]. This function also provides compensation for the phase delay caused by the low-pass filter [8]. To demonstrate the effectiveness of this function, the response of the structure to the same, unrefined digitized impulse ($dt = 4.88E-06s$) was recomputed using all 15 flexible modes. The digitized impulse was then refined by a factor of four ($dt = 1.22E-06s$) and the response recomputed. The FFT was then computed for both responses, as shown in Fig. 8.15.

Figure 8.15 shows that higher order modes exhibited a frequency shift due to the integration process, and that resampling the digitized impulse to a finer time step corrected the distortion. Note that resampling the data to compute the response as described in the previous section was not necessary as the higher order modes contributed very little to the overall response.

However, resampling the data can result in some accumulation of error. Although MATLAB's `resample` function does provide compensation for the phase delay caused by the low-pass filter [8], phase distortion still has an effect on the calibration curve, as shown in Fig. 8.16.

Figure 8.16 shows that some differences in the calibration results exist between the raw and resampled data. Notice that when the full response was included in the calibration curve, the sensitivity did not change but the correlation coefficient diminished slightly from 0.957 to 0.934. When only the trailing end of the response was included in the calibration curve, the raw data actually showed an improvement in correlation from 0.957 to 0.984; however, the resampled data showed a decreased correlation from 0.934 to 0.890 as well as a reduction in the accuracy of the computed sensitivity from less than 1 % error to more than 4 % error. The calibration curves computed using only the trailing portion of the response demonstrate

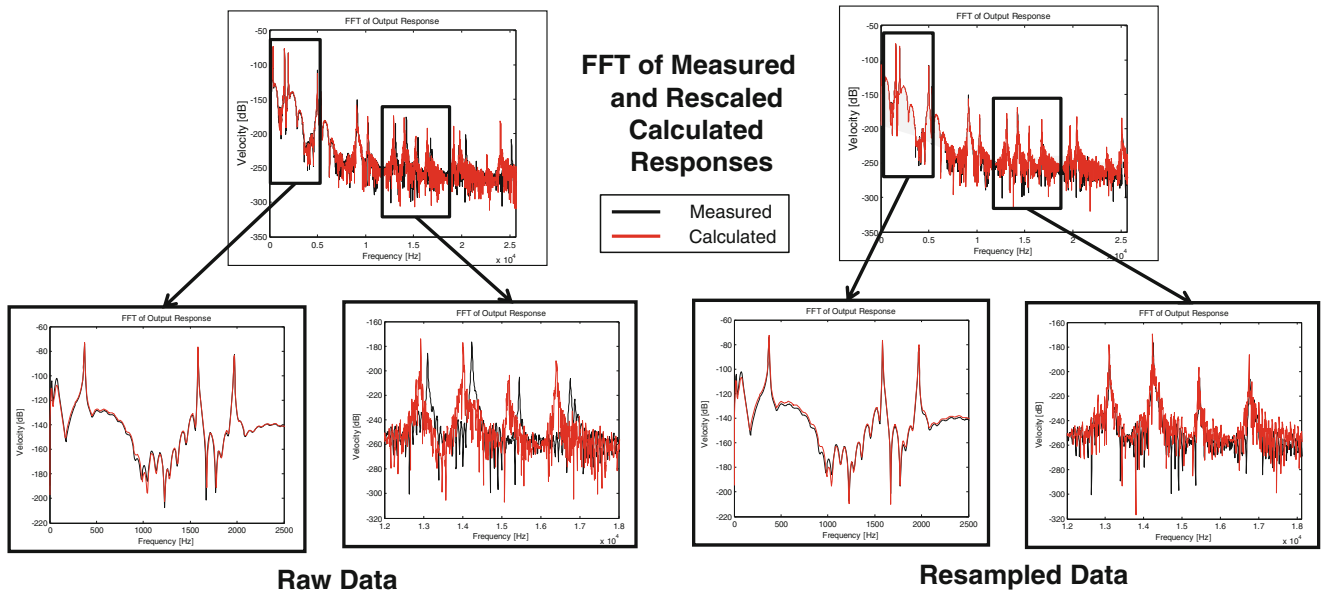


Fig. 8.15 Correction of frequency distortion due to Newmark integration using MATLAB's resample function

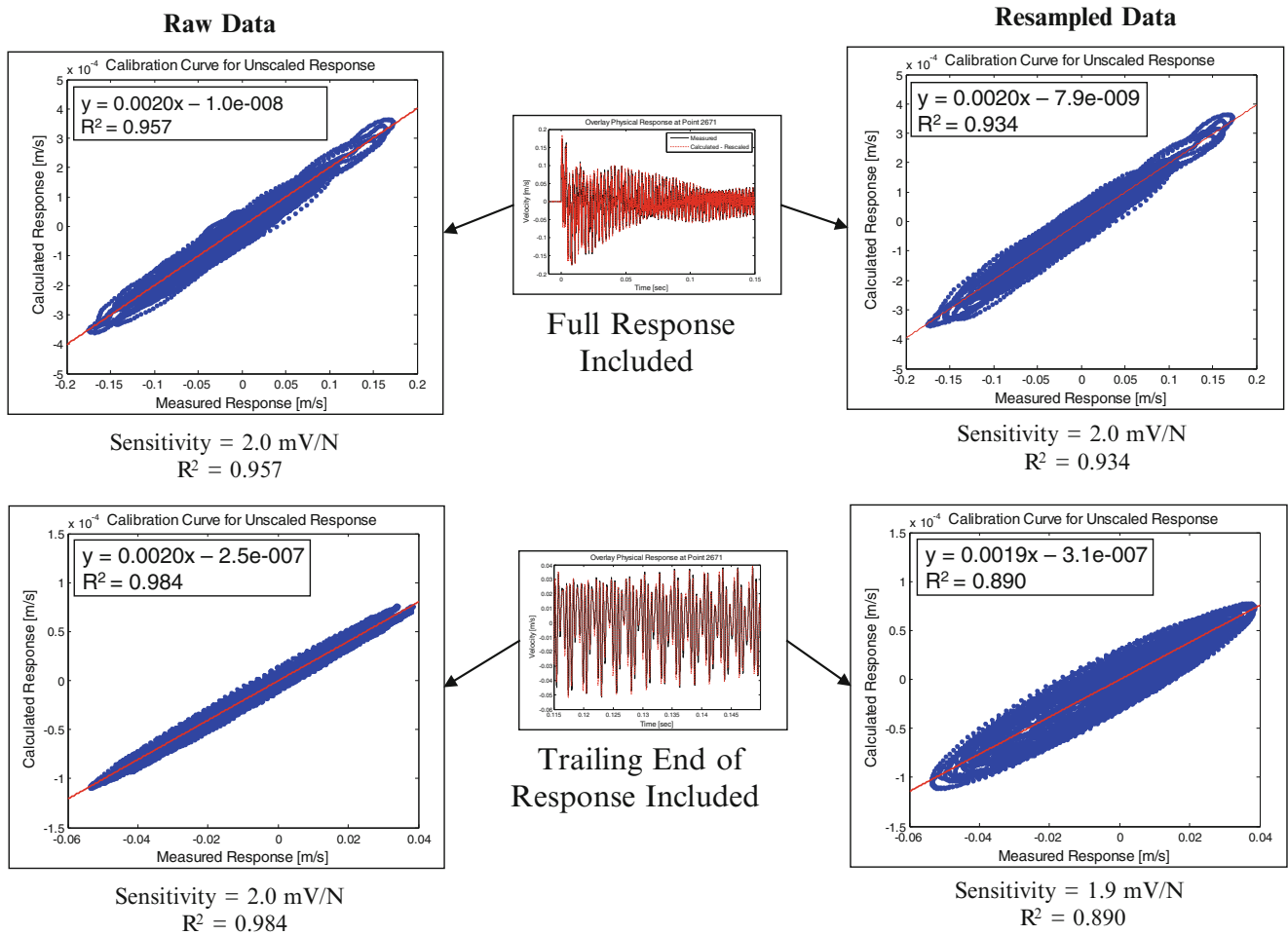


Fig. 8.16 Effect of phase distortion caused by MATLAB's resample function on the calibration curve

that phase distortion was present following MATLAB's resample function. However, most of the higher frequency energy had dissipated by the end of the response indicating that the phase distortion may have been limited to the lower order modes. Investigation into whether this phase distortion will present a problem when extending this calibration method to the ultrasonic transducer is ongoing.

Lastly, the acoustic pressure and subsequently the acoustic force must be characterized for this calibration method to be successful, as the unscaled modal force and input location must be known. Current efforts to characterize this force using both experimental data and simulation are in progress [9].

8.7 Conclusion

The results presented have shown that an analytical model based on the principles of mode superposition can produce an effective representation of a structural response when provided with a digitized input of the excitation. Furthermore, this analytical model has been shown to provide an accurate method of transducer calibration. The measured response from an uncalibrated excitation can be scaled and calibrated using a comparison to the calculated response in order to determine the force applied. The slope of the calculated response versus the measured response provides the unknown calibration. While further investigation is required before extending this calibration approach to an ultrasonic transducer, the preliminary results indicate good accuracy using this method.

Acknowledgements Some of the work presented herein was partially funded by NSF Civil, Mechanical and Manufacturing Innovation (CMMI) Grant No. 1266019 entitled "Collaborative Research: Enabling Non-contact Structural Dynamic Identification with Focused Ultrasound Radiation Force." Any opinions, findings, and conclusions or recommendations expressed in this material are those of the authors and do not necessarily reflect the views of the particular funding agency. The authors are grateful for the support obtained.

References

1. Logan, P., Avitabile, P.: Calibration techniques for non-contacting force excitation part 1. Frequency domain methods. Proceedings of the 34th IMAC. Orlando, FL (2016).
2. Femap—Finite Element Modeling and Postprocessing, Version 10.0.2. UGS Corp.
3. FEMtools 3.8—Dynamic Design Solutions. Leuven, Belgium.
4. Itoh, T.: Damped vibration mode superposition method for dynamic response analysis. *Earthquake Eng. Struct. Dynam.* **2**(1), 47–57 (1973)
5. MATLAB—Matrix Analysis Software. The MathWorks, Inc., Natick MA.
6. Polytec Scanning Laser Doppler Vibrometer. Polytec. Opt. Meas. Syst.
7. LMS Test. Lab—Leuven Measurement Systems, Leuven, Belgium
8. The Mathworks, Inc.: Signal processing toolbox: user's guide (r2015b). http://www.mathworks.com/help/pdf_doc/signal/signal_tb.pdf (2015). Accessed 16 Sept 2015.
9. Chen, S., Niezrecki, C., Avitabile, P.: Experimental mapping of the acoustic field generated by ultrasonic transducers. Proceedings of the 34th IMAC. Orlando, FL (2016).